CAVITATION TUNNEL TESTS FOR PROPELLER NOISE OF A FRV AND COMPARISONS WITH FULL-SCALE MEASUREMENTS

M. Atlar, A.C. Takinaci, E. Korkut
University of Newcastle upon Tyne, UK

N. Sasaki and T. Aono
Sumitomo Heavy Industries, Japan

Abstract

This study presents the results of cavitation tunnel tests carried out with model propeller of a Fisheries Research Vessel (FRV) and those of noise measurements with its full-scale propeller to validate the low-noise performance of this propeller. The tests involve the simulation of a target wake using a wake screen and the determination of the nature and extent of the observed cavitation behind the simulated wake. The measurements for the noise levels of the model propeller and their analyses are also part of the study. The net noise levels of the model propeller are extrapolated to full-scale using the scaling law recommended by the 18th ITTC Cavitation Committee. The extrapolated results are compared with the criteria recommended by the International Council for the Extrapolation of the Sea (ICES) as well as against the full-scale measurements carried out with this vessel in Japan.

1 Introduction

In the design of naval or research vessels, reduction of underwater noise radiated from the vessel is of primary importance for the reliable operation of onboard acoustic instruments. Considerable part of noise generated by the ship system is the underwater noise and the major sources contributing to this are due to the machinery, propeller and background hull flow noise as described by Ross (1976). Amongst these sources the propeller noise, particularly for the cavitating propeller, is the most harmful one for acoustic survey operations since the dominant noise levels can cover a wide frequency band, as reported e.g. Sasajima et al (1986). Therefore the design of low noise propellers for these types of vessels is utmost important and requires feedback from model tests in cavitation tunnels.

This study presents the details and results of the recent cavitation tunnel tests and full-scale noise measurements to validate the design of a 4 bladed and low noise CPP propeller of 39*m* Fisheries Research Vessel (FRV). In order to achieve the objectives of such a validation study, there is no doubt that, there are number of state-of-the-art very large cavitation tunnels, where the entire hull model with its appendages and propeller of respectable size can be fitted, and the associated cavitation and noise tests could have been performed. While this is highly desirable, the time and cost of these tests will be accordingly high. Alternatively medium size cavitation tunnels, where either a "dummy hull" with wake screen or only a wake screen is used for the target wake simulation, can provide more rapid and economical solution. Of course the experience of each tunnel facility in extrapolating the model tests results to full-scale is the key factor in both options beside sound recommendations for the extrapolation and wealth of available full-scale data which are scarce, particularly, for propeller noise.

Within the above framework, the main objectives of this study is to demonstrate the practical worthiness of medium size cavitation testing facilities in predicting the acoustic characteristics of a noise sensitive propeller and to provide useful propeller noise data in full-scale. The details of the model tests, full-scale measurements and comparisons of the model test based predictions with the full-scale noise data the other objectives of the study.

The cavitation tunnel tests, which were carried out at Emerson Cavitation Tunnel (ECT) of Newcastle University, involved the simulation of a target axial wake using 2-D wake screen and the observation of cavitations with 300*mm* brass model propeller for eight different operating conditions behind the simulated wake. The details of the propeller design and model propeller, wake simulations and cavitation tests are given in Section 2, 3 and 4 of the paper

respectively. The noise level measurements by a single miniature hydrophone for different operating conditions and the extrapolation of the net propeller noise to full-scale using the scaling law recommended by the 18th ITTC Cavitation Committee (1987) are presented in Section 5. The comments on the full-scale noise level with regard to the criteria recommended by the International Council for the Extrapolation of the Sea (ICES) are given in Section 6. The details of the field measurements carried out at Tateyama Bay of Tokyo and presentation of the results are given in Section 7. While the comparisons of the full-scale noise level with the extrapolations based on the model tests are presented in Section 8, the paper concludes with the overall conclusions obtained from the study given in Section 9.

2 Propeller Design and Model propeller

The principal dimensions of the vessel and propeller, which were designed and built by Sumitomo Heavy Industries (SHI), are included in Table 1.

Table 1. Main particulars of the propeller and vessel

Propeller		**Vessel**	
Number of Blades	4	Length between perpendicular	33.5 *m*
Propeller Diameter	2.1 *m*	Breadth	7.8 *m*
Pitch Ratio at 0.7R	0.8464	Draught without trim	3.0 *m*
Expanded Blade Area Ratio	0.55	Initial Trim	1.0 *m*
Boss Ratio	0.276	Block Coefficient	0.579
Rake	0 Degrees		
Skew	40 Degrees		
Direction of rotation	Right handed		

In order to minimise the propeller radiated noise, a trade-off design between the efficiency and low noise requirements was applied by SHI to design the propeller, as well as the hull, taking into account the uniform wake distribution. Figure 1 shows the wake distribution measured by the tank tests with 3.7*m* long model, which displayed excellent wake uniformity due to the well-designed stern form.

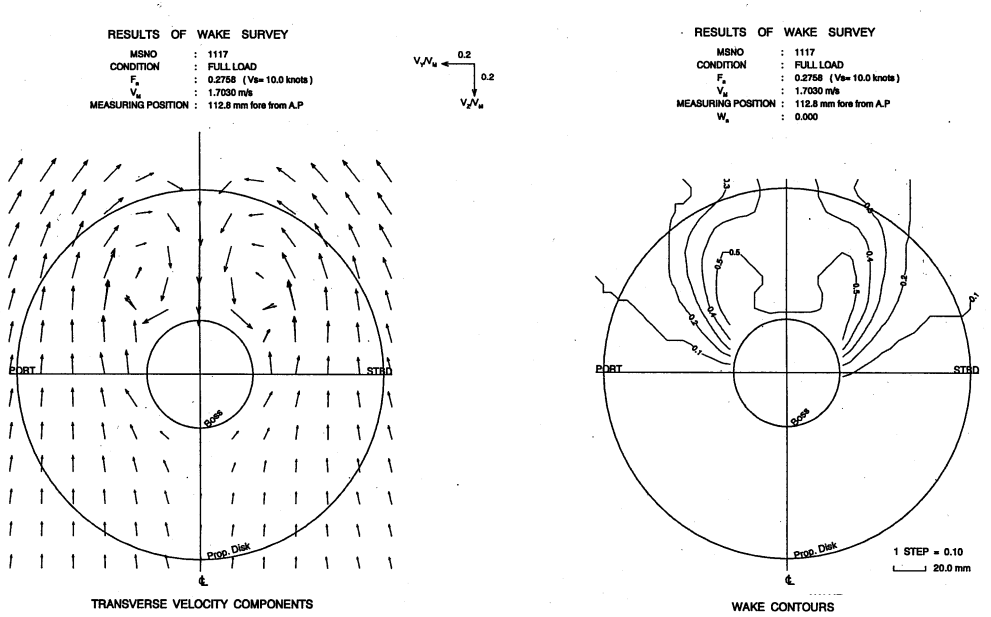

Figure 1: Wake distribution based on model tests at 10 *knots* design speed

The extent of the propeller cavitation was predicted by an in-house computer code at SHI based on QCM (Quasi-Continuous-Method). As shown in Figure 2, and confirmed by the cavitation tunnel tests later in Section 4, it was revealed that cavitation free condition could be obtained up to 10*knots*.

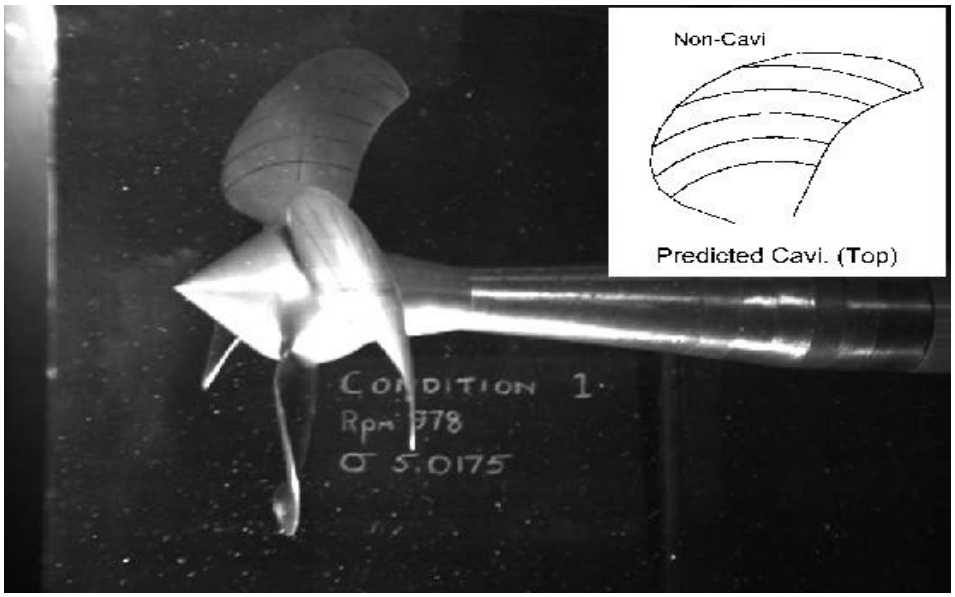

Figure 2: Comparison of cavitation pattern predicted by calculation using QCM method and model tests at 10 *knots* design speed.

In order to have a relatively large Reynolds number, the model diameter was decided to be 300 *mm* which provided a scale factor (*l*) of 7. Although the full-scale propeller has controllable pitch, the model was manufactured as a mono-block with a fixed pitch as requested by the customer. The model material was brass and, tolerances and surface finish were suitable for noise measurements. As shown in Figure 3, the radial lines *r/R*=0.5, 0.6, 0.7,0.8 and 0.9 were marked on each blade as well as the directix for cavitation observations. A cylindrical idle mass with 85*mm* radius and 100*mm* length was also manufactured of brass material to replace the model propeller during the background noise measurements.

Before the tests the hydrodynamic performance prediction was also obtained using an in-house propeller analysis software (Takinaci and Atlar 2001). Figure 3 (right) shows a 3D representation of the model propeller obtained from this software.

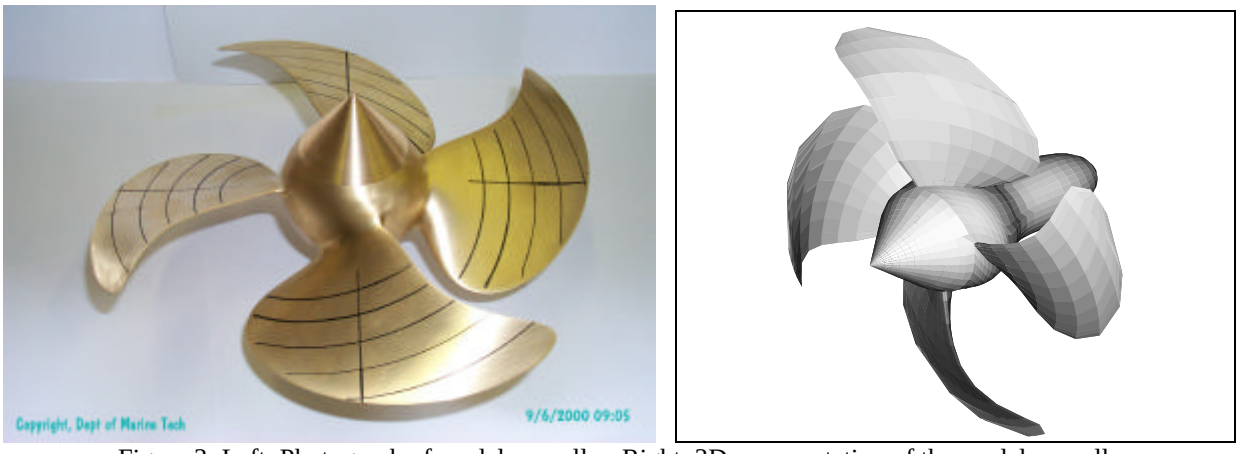

Figure 3: Left: Photograph of model propeller. Right: 3D representation of the model propeller.

3 Wake Simulation Tests

As requested by SHI, the simulation of the wake flow in the axial direction only would be adequate for these tests. Therefore, the target wake velocity ratios (V_a/V_s) provided by SHI were simulated using a different size of meshes attached to a square frame and the wake velocities were measured using a pitot static tube comb and "scanivalve" assembly. By following the standard procedure adopted in ECT, a 500*mm*×500*mm* (*B´H*) frame to carry varying size of wire meshes was placed upstream of the propeller at a distance of approximately two times the model propeller diameter. The Pitot tube comb carrying five 2-holed pitot tubes was mounted on the shaft of K&R H33 dynamometer downstream of the frame. When carrying out the wake survey the velocity was obtained from the readings of total and static head pressures experienced by each of the five pitot tubes. Each pressure reading was switched by the scanivalve assembly to the pressure transducer to obtain the respective output, which was converted to the required velocity using the Bernoulli Equation. The tunnel water speed used during the wake survey was kept at 3 *m/s* and the velocity measurements were taken at the fractional radii of *r/R*=0.3, 0.5, 0.7, 0.9 and 1.1.

The wake survey was carried out five times with successive modifications of the mesh screen, until the differences between the target and achieved wake velocities were acceptably small. The comparisons of the wake velocity ratios (i.e. 1-*w*= V_a/V_s) for the target and the achieved wake at fractional radius of 0.7 and 0.9 are shown in Figures 4 and 5 as example. In the figures 0° (and 360°) degrees corresponds to the Top Dead Centre (TDC) of the propeller plane whereas 180° corresponds to the Bottom Dead Centre (BDC). In overall the calculated difference in values of the mean wake flow velocity ratio (1-*w*) for the target and achieved wake flow was 2.23% over the propeller disk and this was found to be satisfactory for these tests

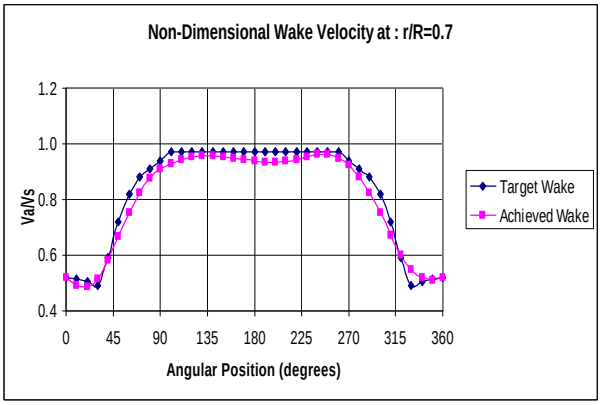

Figure 4: Comparison of wake velocity ratios of the target and the achieved wakes for radial fraction *r/R*=0.7.

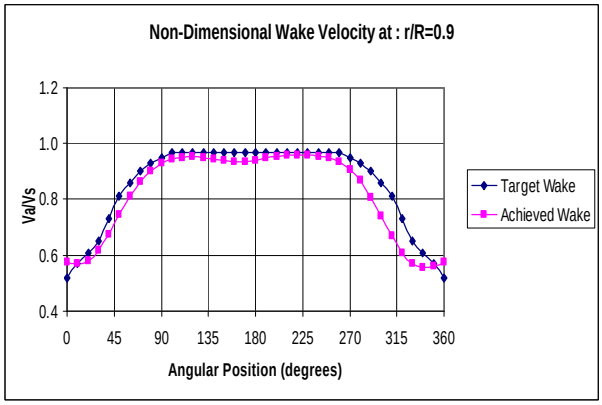

Figure 5: Comparison of wake velocity ratios of the target and the achieved wakes for radial fraction *r/R*=0.9.

4 Cavitation Tests

4.1 Set up and Test Conditions

Following the wake simulation tests, the propeller model was mounted on the K&R H33 dynamometer downstream of the wake screen. In order to provide clear visibility for the cavitation observations and video filming, it was decided to keep the tunnel under a moderate amount of reduced pressure, which was achieved by applying vacuum to the tunnel, at 0.3 *mHg* (mercury) of constant value for all testing conditions. Under the effect of this constant pressure, in order to meet the operating conditions, which is shown in Table 2, the model propeller rate of revolution (*N*) was adjusted to satisfy the required cavitation numbers (s_n) using equation 1 while the tunnel impeller speed was adjusted until the water speed corresponded to the respective thrust coefficient K_t for each condition.

The above approach resulted in the testing conditions for the model propeller rpm and thrust values presented in the last two columns of Table 2. The water speed of the tunnel varied between 2.66 *m/s* and 4.8 *m/s* in order to satisfy the K_t values required.

Table 2 Summary of testing conditions (*).

No	Operating Condition	Ship Speed (*knots*)	K_t	s_n	*N(rpm)* (model)	*T(N)* (model)
1	K_t	10	0.1382	5.0175	978	298
2	K_t * 0.8	10	0.1106	5.0175	978	238
3	K_t * 1.2	10	0.1658	5.0175	978	357
4	s_n * 0.9	10	0.1382	4.5158	1031	331
5	Maximum Speed	13.2	0.1751	2.2031	1476	860
6	K_t * 0.8	13.2	0.1401	2.2031	1476	688
7	K_t * 1.2	13.2	0.2101	2.2031	1476	1032
8	s_n * 0.9	13.2	0.1751	1.9828	1556	955

(*) The tests are performed under a 0.3 mHg constant vacuum for all conditions

In establishing the test conditions in Table 2, the following formulae were used for s_n and K_t.

$$s_n = \frac{P_{atm} + H_{st}\, g\left(r_{Hg} - r_w\right) - P_V}{\frac{1}{2} r_w n^2 D^2} \tag{1}$$

$$K_t = \frac{T}{r_w n^2 D^2} \tag{2}$$

where P_{atm} is the atmospheric pressure read at the tunnel barometer (in N/m^2), H_{st} is the static pressure at the tunnel manometer (in N/m^2), g is the gravitational acceleration (in m/s^2), r_{Hg} is the mass density of mercury in the tunnel manometer (in kg/m^3) and r_w is the mass density of the tunnel solution (in kg/m^3). P_V is the saturated vapour pressure (in N/m^2), n is the model propeller rate of rotation (in *rps*), D is the model propeller diameter (in m) and T is the model propeller thrust (in N).

One of the important test parameters in the cavitation tests and consequently in the noise measurements is the amount of the total gas content (a/a_s) in the tunnel solution. For accurate extrapolation of the tunnel results to the full-scale, the gas content of the solution should be fully saturated to correspond with that of seawater. As the normal practice in ECT for efficient observation of the model propeller cavitation, a gas (oxygen) content ratio $a / a_s \leq 0.6$ is required for relatively high cavitation numbers.

In these tests the total gas content of the water was decided to be kept at a/a_s=0.5 corresponding to the saturation at the tunnel working pressure. However, the measurement of the gas content would require "Van Slyke" apparatus. Since the use of this type of device, which contains mercury, has now been banned in the university due to health hazards, the dissolved gas content of the tunnel solution was measured using a Jenway DO_2 meter 9071 apparatus. The existing calibration curve between the total gas content and the dissolved oxygen indicated that the necessary oxygen level would be around 0.3 to correspond to 0.5 total gas content. Therefore, a 30% dissolved oxygen level was kept throughout the entire cavitation tests and noise measurements as practical as possible. This required long duration for the de-aeration process, filtering and frequent controls of the water quality during the tests.

4.2 Cavitation and Pattern Observations

The cavitation observations were made under stroboscopic lighting for the eight conditions as shown in Table 2. Video recordings and captured images were also taken using a high speed CCD (Flashcam) video camera with a fast electronic shutter, which can be triggered at any time yielding an imaging frequency of 0 to 50 *frame/s*.

The appearance of the cavitation patterns for the first four conditions are restricted to a very fine, unattached fluctuating tip vortex mainly around the propeller's top dead centre. The tip vortex could be traced for 7 to 8 revolutions downstream of the propeller and less than a mm thickness. In condition 5 through 8, the propeller blades developed steady tip vortices around the clock as well as developing fluctuating ($0.7<r/R<0.9$) to steady

(0.8<*r/R*<1.0) sheet cavitation with increasing extent moving from condition 5 towards condition 8 restricted to ±20°-30° around the TDC. The extent of the vortex cavitation could be traced downstream of the propeller for more than 10 revolutions with increasing thickness, which could reach 2-3 *mm*. While the above is the summary of the cavitation patterns some times a very fine and hardly visible misty cavitation, which could be associated with the flow separation, was observed off the trailing edges of the blades (0.7<*r/R*<1.0) for the last three conditions. Finally, the extension of the sheet cavitation and the tip vortex cavitation around the tip of the blade displayed a resulting twisted tip vortex in the downstream and around ±20° from the top dead centre. However, none of the above cavitation patterns appeared to cause any serious cavitation damage to the propeller or its performance. In Figures 6 and 7 the cavitation sketches are shown for a reference blade around ±20°-30° from the TDC (i.e. 0°) for all the tests condition to present the nature of the cavitation patterns. On the other hand, photographs that illustrate the captured video images of the reference blade around the TDC for each condition tested to provide further insight into the nature of the cavitation can be obtained from Takinaci et al (2000).

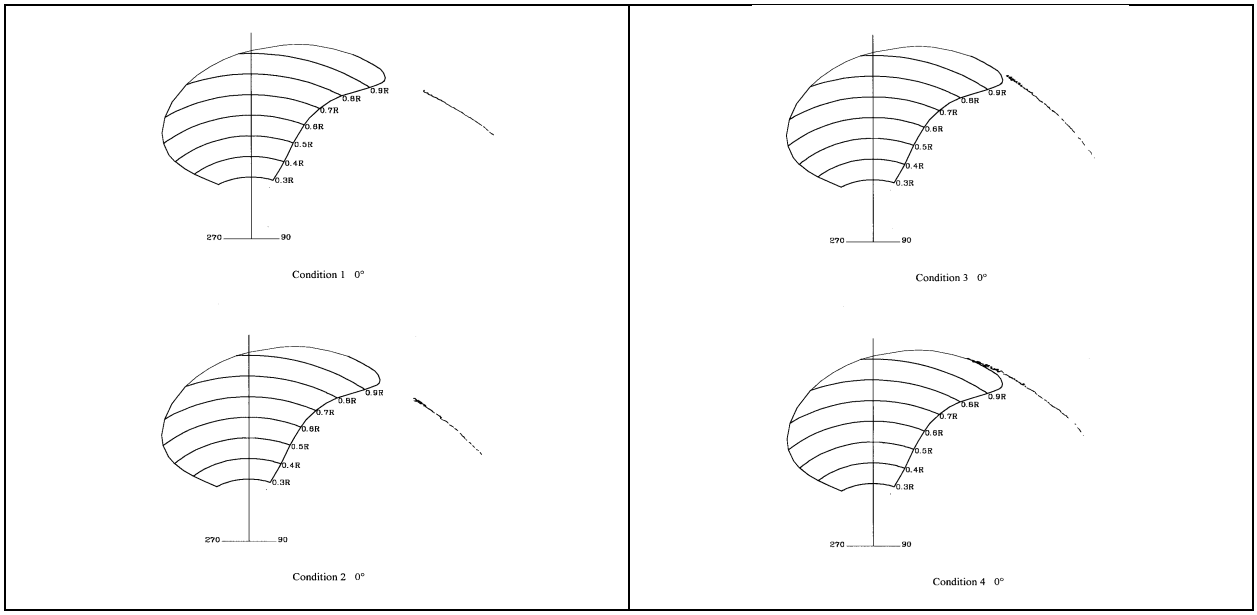

Figure 6: Cavitation sketches for. Left: Conditions 1 and 2. Right: Conditions 3 and 4.

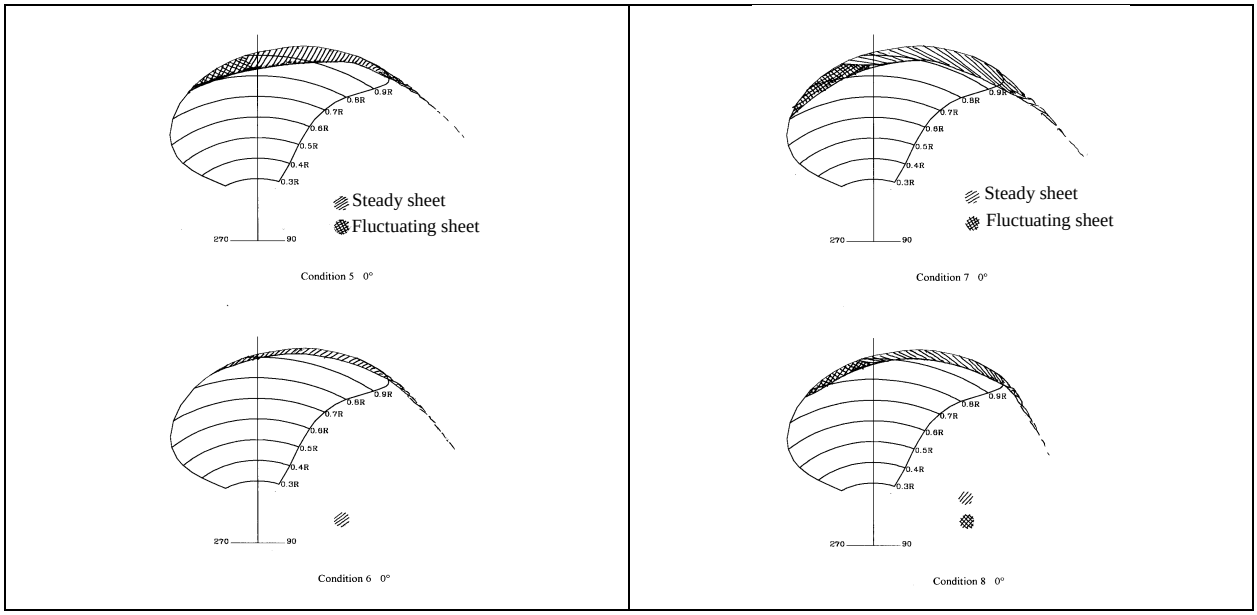

Figure 7: Cavitation sketches for. Left: Conditions 5 and 6. Right: Conditions 7 and 8.

5 Noise Measurements

5.1 Set-up and Test Conditions

The same experimental set-up used in the cavitation tests was applied for the noise measurements. However, the noise measurements were made for only the first five of the eight conditions specified for the cavitation tests. These conditions are re-stated including the tunnel speed as shown in Table 3.

Table 3. Full-scale and corresponding test conditions for noise measurements.

No	Operating Condition	Ship Speed (*knots*)	K_t	s_n	*N(rpm)* (model)	*N(rps)* (model)	*T(N)* (model)	*V* (*m/s*) (Tunnel speed)
1	K_t	10	0.1382	5.0175	978	16.31	298	3.00
2	K_t * 0.8	10	0.1106	5.0175	978	16.31	238	3.35
3	K_t * 1.2	10	0.1658	5.0175	978	16.31	238	2.66
4	s_n * 0.9	10	0.1382	4.5158	1031	17.18	331	3.20
5	Maximum Speed	13.2	0.1751	2.2031	1476	24.60	860	4.05

Noise levels were measured by means of a single Bruel & Kjaer Type 8103 Miniature Hydrophone situated in a water-filled, thick-walled, steel cylinder placed on a 30 *mm* thick Plexiglas window above the propeller at a vertical distance of 405 *mm* from the shaft centre line of the dynamometer. Signals from the hydrophone were collected and analysed by means of further Bruel & Kjaer equipment, viz. a type 2636 Charge Amplifier, a type 2610 Measuring Amplifier and a Type 1617 1/3 Octave Band Pass Filter, the latter comprising 1/3 Octave bands with centre frequencies ranging from 2 *Hz* to 160 *kHz*. As stated in the cavitation tests, the dissolved gas content of the tunnel solution was kept at 30% during the noise measurements. Using the above-described equipment and test conditions, the noise levels of the propeller were recorded at centre frequencies ranging from 50 *Hz* to 160 *kHz*. During the recordings the measurements were taken three times for each centre frequency and the mean value of the measurements were accepted as the final recording. In the first set of measurements the noise measured was the total noise, including both the net propeller noise and the noise generated by the proximity (background noise). Consequently, in order to calculate the noise generated exclusively by the propeller, i.e. the net propeller noise, the background noise had to be measured and subtracted logarithmically from the total noise. During the noise measurements the selected range of the tunnel water speed and relatively large diameter of the propeller provided a Reynolds number range of $1.30\times10^6<Rn_{0.7R}<1.95\times10^6$ where Reynolds number is defined as

$$Rn_{0.7R} = \frac{V_{0.7R}\, C_{0.7R}}{n} \tag{3}$$

where $V_{0.7R}=[V^2+(0.7\pi nD)^2]^{1/2}$, D=0.30 *m*, $C_{0.7R}$ is the chord length at *r/R*=0.7 ($C_{0.7R}$=0.1136 *m*) and n is the kinematic viscosity.

After the total noise level measurements, following the standard procedure applied in the ECT, the background noise of the tunnel was measured. In the second set of measurements the earlier described idle mass replaced the model propeller and the tunnel was kept working at the same operating condition having the same water quality as for the total noise measurements carried out previously.

5.2 Analysis and Presentation of Results

A common practice in the analysis and presentation of the noise levels is to reduce the measured values of Sound Pressure Levels (*SPL*) in each 1/3 Octave band to an equivalent 1 *Hz* bandwidth by means of the correction formula recommended by ITTC (1978) as follows.

$$SPL_1 = SPL_m - 10\log Df \tag{4}$$

where SPL_1 is the reduced sound pressure level to 1 *Hz* bandwidth in *dB*; re 1 *mPa*, SPL_m is the measured sound pressure level at each centre frequency in *dB*; re 1 *mPa* and *Df* is the bandwidth for each one-third octave band filter in *Hz*.

The ITTC also required that the sound pressure levels be corrected to a standard measuring distance of 1 *m* using the following relationship.

$$SPL = SPL_1 + 20\log(r) \tag{5}$$

where *SPL* is the equivalent 1 *Hz* at 1 *m* distance sound pressure level (in *dB*; re 1 *mPa*) and *r* is the vertical reference distance for which the noise level is measured (*r*=0.405 *m*). Having converted the measured *SPL*s for the total and the background noise to the equivalent 1 *Hz* at 1 *m SPL*s using equations 4 and 5, the level of net sound pressure of the propeller (SPL_N) at each centre frequency was calculated using the following logarithmic subtraction formula given by Ross (1976).

$$SPL_N = 10\log\left[10^{\left(SPL_T/10\right)} - 10^{\left(SPL_B/10\right)}\right] \tag{6}$$

where SPL_T is the total sound pressure level measured at an equivalent 1 *Hz* bandwidth and 1 *m* (in *dB*; re 1 *mPa*). SPL_B is the background sound pressure level measured at an equivalent 1 *Hz* bandwidth and 1 *m* (in *dB*; re 1 *mPa*). The results of the net sound pressure levels are also presented in Figures 8 through 10. In these figures, the logarithmic-scaled *x*-axis represents the centre frequencies in *Hz* while the linear-scaled *y*-axis represents the sound pressure levels in *dB*; re 1 *mPa*, 1 *Hz*, 1 *m*. In Figures 8 through 10, the dotted lines in the low to medium range of the frequency band indicate the regions where the measured background noise levels were higher than the level of the propeller noise. According to equation 6, since the negative logarithmic values would not make sense it was decided to present the total sound pressure levels in those regions rather than leaving it blank.

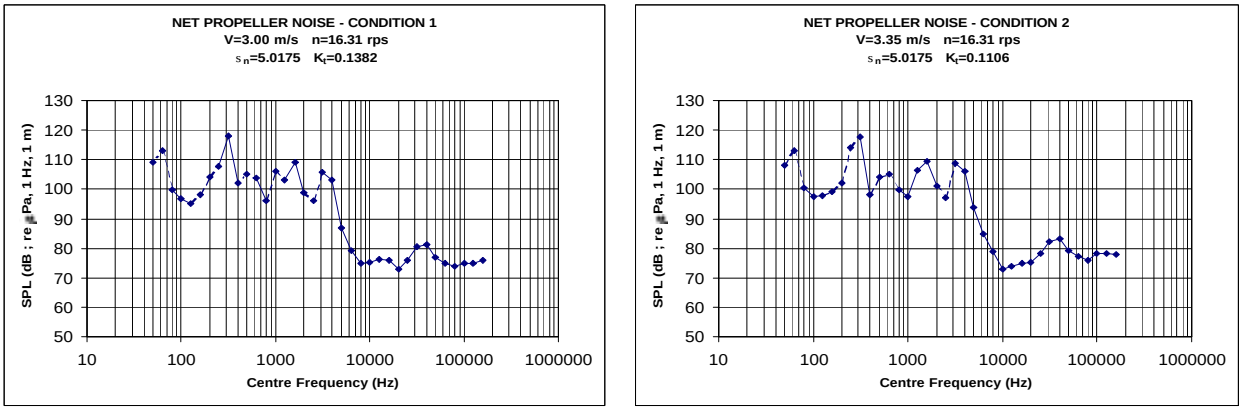

Figure 8: Model propeller noise level spectra. Left: Condition 1. Right: Condition 2.

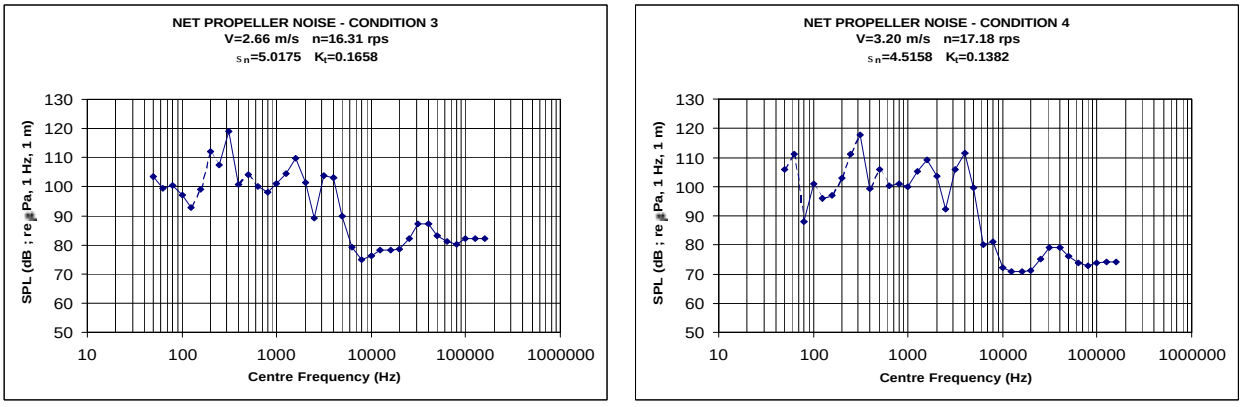

Figure 9: Model propeller noise level spectra. Left: Condition 3. Right: Condition 4.

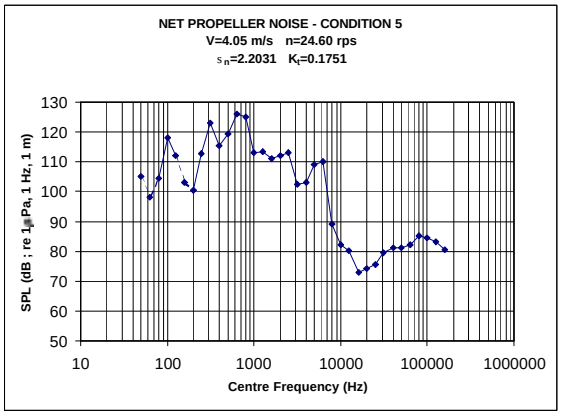

Figure 10: Model propeller noise level spectra for condition 5.

6 Comments on Full Scale Noise Level with Regard to ICES

The ship owner required that the full-scale propeller noise should conform to the criteria recommended by the International Council for the Exploration of the Sea (ICES) at 10 *knots* at calm and deep open sea and straight ahead free running condition.

Although there are some scaling procedures applied to obtain full-scale noise level of a propeller based on model tests (e.g. Levkovskii 1968; Bjorheden and Astrom 1977; Lovik 1981; Bark 1982 and 1992, etc.), predictions usually give higher levels of noise than the full-scale measurements. This can be explained by that model noise tests are usually carried out in a highly reverberant environment (high level of background noise due to the dynamometer, impeller, etc.) and causing the difficulty in interpreting the genuine propeller noise as well as other factors (i.e., dissolved gas content, viscosity, etc.) (ITTC 1987). Therefore accurate prediction of full scale propeller noise from model tests carried out in a cavitation tunnel is impossible without detailed knowledge of the influence of the proximity of the tunnel walls and other factors which might affect the scaling from model to full scale. The determination of correlation factors to be applied to model measurements would involve a large programme of model and full-scale tests. For this reason, such correlation factors do not exist for the Emerson Cavitation Tunnel.

However, an approximation to the full-scale noise levels has been made using scaling laws recommended by the Cavitation Committee in ITTC (1987). These laws are concerned only with differences in dimensions and operating conditions of the model and full scale propellers and take no account of the fact that the model measurements may have been made in a cavitation tunnel.

The increase in noise in moving from model to full scale is given by,

$$DL_{(P)} = 20\,log\left[\left(\frac{D_P}{D_M}\right)^z\left(\frac{r_M}{r_P}\right)^x\left(\frac{s_P}{s_M}\right)^{y/2}\left(\frac{n_P D_P}{n_M D_M}\right)^y\left(\frac{r_P}{r_M}\right)^{y/2}\right] dB \qquad (7)$$

and the frequency shift

$$\frac{f_P}{f_M} = \frac{n_P}{n_M} \qquad (8)$$

In the above, the subscripts *P* and *M* refer to the ship and model respectively, *D* is the propeller diameter which is equal to 2.1 *m* for the ship and 0.3 *m* for the model, *r* is the reference distance for which the noise level is predicted and is equal to 1 *m* for both ship and model, *s* is the cavitation number which has the same value for ship and model, *n* is the propeller rate of rotation and *r* is the mass density of water which has a measured value of 1002

kg/m^3 for the cavitation tunnel and assumed standard value of 1025.9 kg/m^3 for the sea water. With these values and putting y=2 and z=1, the expression for the increase in noise level reduces to

$$DL_{(P)} = 20\,log\left[351.18\left(\frac{n_P}{n_M}\right)^2\right]dB \tag{9}$$

For conditions 1, 2, 3 and 5, $n_P/\ n_M$=0.2014. The frequencies are reduced in that ratio and noise levels are increased by 23 *dB*. For condition 4, the corresponding values are 0.1911 and 22 *dB*.

The full-scale noise levels derived in this manner from the model results are given in Figures 11 through 13 in comparison with lines representing the ICES recommended levels. On model scale, the maximum measurable centre frequency is 160 *kHz*, which on scaling reduces to about 32 *kHz*. Because of the doubts discussed above regarding the scaling procedure, it is difficult to comment on these results and draw firm conclusions from them. For conditions, 1 to 4 there is a clear peak value at a frequency approximately equal to 5 x Blade Rate Frequency. This could be due to the incipient and fluctuating tip vortex cavitation, which was observed during those tests. In each case, the noise level tends to rise above the ICES level in the region of 20 *kHz* to 30 *kHz* i.e. towards the upper limit of measurable spectrum. Condition 5 shows much higher noise levels reflecting the more extensive cavitation in that condition.

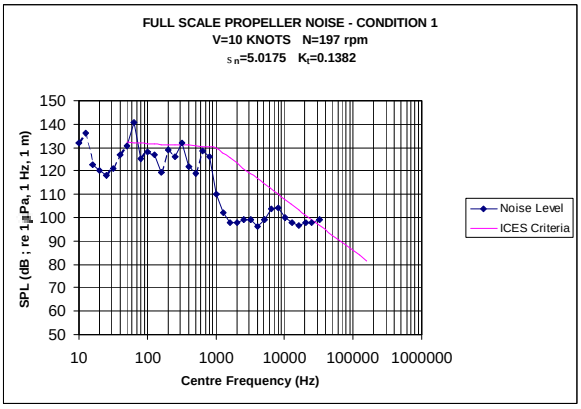

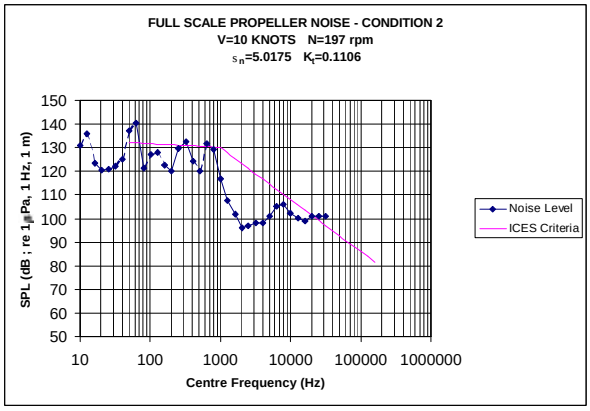

Figure 11: Full-scale propeller noise level spectra for. Left: Condition 1. Right: Condition 2.

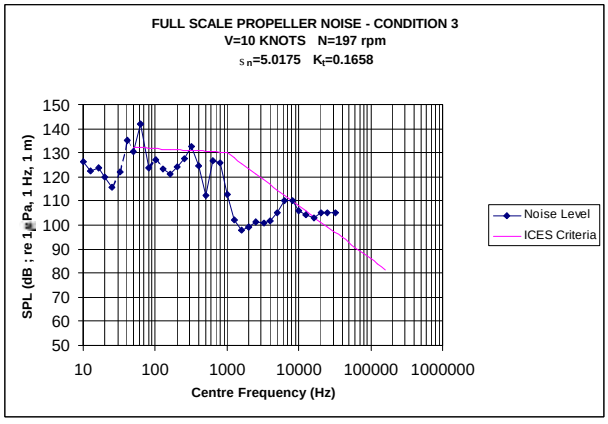

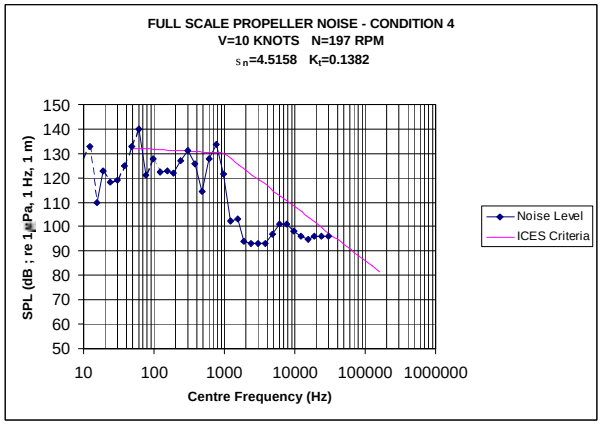

Figure 12: Full-scale propeller noise level spectra for. Left: Condition 3. Right: Condition 4.

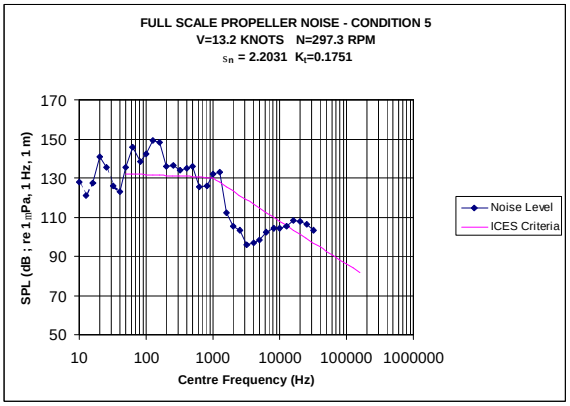

Figure 13: Full-scale propeller noise level spectra for Condition 5.

7 Full Scale Measurements

7.1 Set-up and Test Conditions

The propeller-radiated noise of the FRV was measured at off Tateyama Bay of Japan where the water depth is about 800*m* deep. A single B&K 8104 type hydrophone was suspended at a depth of 17.5*m* from a buoy, which was located at a distance of abt. 50*m* from the sailing line of the FRV, as shown in Figure 14. The accurate values of the distance between the vessel and hydrophone were obtained from the signal of the differential GPS used.

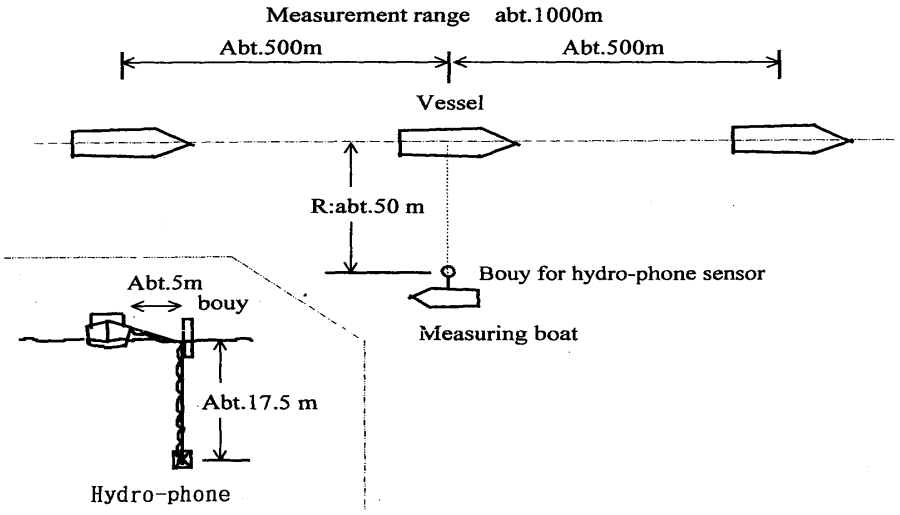

Figure 14. Test arrangement of the full-scale noise measurements

Total number of test conditions was seven and five of these are given in Table 4. Since the FRV had a controllable pitch propeller, one can see the effect of ship speed by comparing test condition A and C at the ordinary design pitch (21 *deg*) while test case E represents higher loading condition at relatively low pitch angle (17.5 *deg*)

Table 4. Full-scale test conditions

Test case	**Propeller Pitch (*deg*)**	**Speed *knots*)**	***N (rpm)***	K_t	s_n
A	21	9.0	182	0.118	5.514
B	22	9.4	182	0.105	5.514
C	21	9.6	192	0.115	4.955
D	22	9.9	191	0.105	5.007
E	17.5	11.6	272	0.155	2.470

7.2 Analysis and Presentation of Results

It is generally recognized that propeller radiated noise from the vessel can be assumed to have spherical spreading characteristics and therefore the measured noise levels are corrected according to the following equations assuming that the transmission loss is proportional to the square of the distance:

$$TL = 20\ log\ (R/R_0) \tag{10}$$

where TL is the transmission loss and R is the distance between hydrophone and the propeller position, $R_0 = 1\ m$. The analysed results for the five test conditions including the ICES Criteria are presented in Figure 15, where the y-axis is the full scale Sound Pressure levels in *dB*; re 1 *mPa*, 1 *Hz*, 1 *m*, while the logarithmic x-axis represents the centre frequencies in *Hz*.

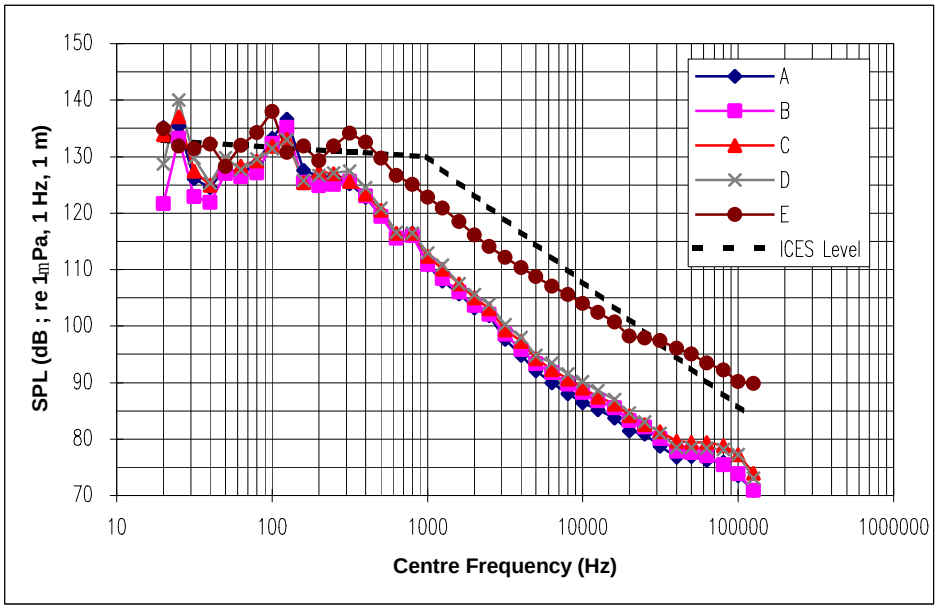

Figure 15: Full-scale noise measurements in various conditions

8 Comparison with Full Scale Measurements

By considering the five sets of the full-scale noise measurements and those of the model test based predictions, it appears that full scale case for "Test C" can be compared with the model test based prediction for " Condition 2", while the remaining conditions have relatively different operating conditions (i.e. K_t and s_n). Therefore Figure 16 shows the comparable two cases (i.e. Test C and Condition 2) including the ICES recommendation level.

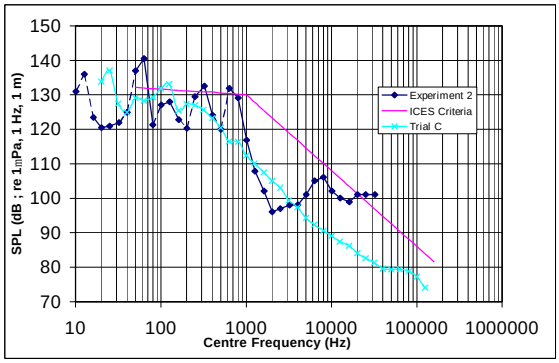

Figure 16. Comparison of noise predictions with full-scale measurements (Kt ~ 0.11, s_n ~5.0)

As shown in Figure 16 general correlation between the full-scale measurement and the prediction appears to be good except in the high frequency region. The prediction displays a sharp increase at the tail end of the frequency region and this can be attributed to the collapse behaviour of the bubbles stimulated by the wire meshes used for the wake simulations. Similar behaviour was also observed in the noise tests with Meridian type model propeller where similar meshes were used to vary the free-stream turbulence level of the tunnel water (Korkut (1999) and Korkut et al (2000)). On the other hand, as discussed in Section 6, the predictions are slightly greater than the full-scale measurements due to the reverberant environment of the cavitation tunnel requiring careful analysis of the background noise characteristics of the tunnel.

9 Conclusions

This paper presents some useful model and full-scale data for the cavitation and noise characteristics of a low-noise FRV propeller in complementing the current state-of-the-art design and performance studies of this type of propeller.

- The experimental validation study carried out in the Emerson Cavitation Tunnel has confirmed the low noise performance of the SHI designed propeller to achieve its design objective based on the ICES criteria.
- Beside other routine investigations, medium size cavitation tunnels can provide rapid and economical means to provide basis for the noise investigation of propellers using “dummy hulls” and/or wake screens. Depending upon particular tunnel type, the net propeller noise will require special attention to the measurement and analysis of the background noise of these tunnels due their usually reverberant nature.
- The extrapolation procedure recommended by the 18th ITTC Cavitation Committee has provided a useful basis for the prediction of noise in full-scale for the particular low-noise propeller reported in this paper.

Acknowledgements

The Authors gratefully acknowledge the contributions from Dr. EJ Glover and Mr Ian Paterson, who is the supervisor of the Emerson Cavitation Tunnel, in carrying out the project on which this paper is written.

References

Bark, G. (1982). *Prediction of cavitation noise from two alternative propeller designs-model tests and comparisons with full-scale results*. 1982 ASME Summer Meeting, Arizona, USA.

Bark, G. (1992). *On the scaling of propeller cavitation noise with account of scale effects in the cavitation noise*. International STG-Symposium on Propulsors and Cavitation, Hamburg, Germany.

Bjorheden, O. and Astrom, L. (1977). *Prediction of propeller's noise spectra*. Hydrodynamics of Ship and Offshore Propulsion Systems, Oslo, Sweden, 104-121.

ITTC (1978). *Cavitation committee report*, 15th International Towing Tank Conference, The Hague, The Netherlands.

ITTC (1987). *Cavitation committee report*, 18th International Towing Tank Conference, Kobe, Japan.

Ross, D. (1976). *Mechanics of underwater noise*, Pergamon Press, NewYork, USA.

Korkut, E. (1999). *An investigation into the scale effects on cavitation inception and noise in marine propellers*. Ph.D. Thesis, University of Newcastle upon Tyne, UK.

Korkut, E., Atlar, M. and Odabasi, A.Y. (2000*). Effect of the viscous scale on the inception of cavitation and noise of marine propellers*. International Conference on Propeller Cavitation NCT’50, Newcastle upon Tyne, UK.

Levkovskii, Y.L. (1968). Modelling of cavitation noise. *Soviet Physics-Acoustics*, **13**, 337-339.

Lovik, A. (1981). *Scaling of propeller cavitation noise*. Noise Sources in Ships1: Propellers, Nordforsk, Sweden.

Sasajima, T, Nakamura, N. and Oshima, A (1986). *Model and full scale measurements of propeller cavitation noise on an oceanographic research ship with two different types of screw propeller*. Bulletin, J. (ed), Shipboard Acoustics. Martinus Nijhoff Publishers, Dordrecht, Netherlands.

Takinaci, A.C., Korkut, E., Atlar, M., Glover, E.J., Paterson, I. (2000*). Cavitation observations and noise measurements with model propeller of a fisheries research vessel*. Department Report No:MT-2000-56, Department of Marine Technology, University of Newcastle upon Tyne, Newcastle, UK.

Takinaci, A.C. and Atlar, M. (2001). On the importance of boundary layer calculations instead of viscous correction in heavily loaded marine propellers while using a surface panel method. *Ocean Engineering*, **28**, 519-536.